Nuclear Engineering and Design 429 (2024) 113640

Contents lists available at ScienceDirect

Nuclear Engineering and Design

journal homepage: www.elsevier.com/locate/nucengdes

Design methodology of multi-hole spargers to prevent steam coalescence at sub-atmospheric pressure

Luca Berti *, Donato Aquaro, Rosa Lo Frano

Department of Civil and Industrial Engineering, University of Pisa, Largo Lucio Lazzarino, 56122 Pisa, Italy

ARTICLE INFO

Keywords:
Direct contact condensation
VVPSS
Sparger design
Unstable regimes
Steam coalescence

ABSTRACT

In case of an in-vessel Loss Of Coolant Accident (LOCA), flash steam can be released in the Vacuum Vessel (VV) of the International Thermonuclear Experimental Reactor (ITER) causing its pressurization. To avoid this, the safety system named Vacuum Vessel Pressure Suppression System (VVPSS) will intervene sending the steam to four Vapour Suppression Tanks (VSTs) through a multi-hole sparger and condenses via Direct Contact Condensation (DCC).

To support the design of the multi-hole sparger, which is a key safety component of VVPSS, at the University of Pisa two testing facilities were designed and built in order to study and qualify the VVPSS, named Small Scale Test Facility (SSTF) and Large Scale Test Facility (LSTF).

During the experimental tests performed using LSTF with a VVPSS multi-hole full scale sparger, under certain conditions, the coalescence of the steam jet plumes resulted in the formation and collapse of large, isolated steam bubbles which produced high pressure loads at low frequency on the structure and flow reversal of the pool water inside the sparger.

To limit these large pressure loads, a methodology is needed to prevent the coalescence of the steam jet plumes.

With this aim, an image analysis of 15 experimental tests performed using SSTF was performed to develop and validate a correlation of the ratio between the maximum radius of the steam jet plumes and the hole diameter. Subsequently, two limiting radii for multi-hole spargers (named r_1 and r_2) were determined which allow avoiding the partial and the transitional complete coalescence of the steam jet plumes when compared to the maximum radius. The proposed methodology is new and quite innovative, and it was applied and validated by using the several videos recorded during the transient test performed using sparger B, consisting of DN450 pipe with 1000 holes.

The correlation estimates that partial coalescence and transitional to complete coalescence regions are avoided when the water subcooling temperature ranges between 37–45 °C and 25–31 °C, respectively, as observed in the recordings of the cameras. Results allow to identify the sparger design dimensions preventing the steam jet plumes coalescence, and avoiding the onset of excessive dynamic loads.

Abbreviations: AHOS, All Hypothesized Operating Scenario; BCO, Bubbling Condensation Oscillation; C, Chugging; CC, Complete Coalescence; CIWH, Condensation Induced Water Hammer; CO, Condensation Oscillation; DCC, Direct Contact Condensation; EBO, Encapsulating Bubble Oscillation; ETT, Experimental Test Tank; IRWST, In-Containment Refueling Water Storage Tank; ITER, International Thermonuclear Experimental Reactor; IOC, Interfacial Condensation Oscillation; LOCA, Loss of Coolant Accident; LOVA, Loss of Vacuum Accident; LLTs, Large Loca Tanks; LSTF, Large Scale Test Facility; NC, No Coalescence; PC, Partial Coalescence; SC, Stable Condensation; SLTs, Small Loca Tanks; SSTF, Small Scale Test Facility; TC, Transitional Chugging; TCC, Transitional Complete Coalescence; VSTs, Vapor Suppression Tanks; VV, Vacuum Vessel; VVPSS, Vacuum Vessel Pressure Suppression System.

* Corresponding author.
E-mail address: luca.berti@phd.unipi.it (L. Berti).

https://doi.org/10.1016/j.nucengdes.2024.113640
Received 28 June 2024; Received in revised form 10 September 2024; Accepted 7 October 2024
Available online 15 October 2024

Nomenclature

a_{max}	Maximum Radius Steam Jet plume, m
B	Condensation driving potential
c	Ratio between px and py
D_H	Hole diameter
c_p	Isobaric heat capacity, J/kg K
C_D	Efflux coefficient
G	Steam mass flux
G_c	Critical steam mass flux, kg/m^2 s
G_H	Single hole steam mass flux, kg/m^2 s
h_{fg}	Latent heat of vaporization, J/kg
p_0	Steam Pressure, Pa
p_x	Pitch between holes in the same row, m
p_y	Pitch between holes of different rows, m
r_1	Limit to avoid PC
r_2	Limit to avoid TCC
Greek letters	
γ	Ratio between the specific isobaric and isochoric heat capacity of steam
Δy_{max}	Maximum diameter of steam jet plume, m
ΔT_{sub}	Pool subcooling temperature, °C
ρ_0	Steam Density, kg/m^3

1. Introduction

Direct Contact Condensation (DCC) is a highly efficient heat exchange mechanism. The heat transfer coefficient at the interface between steam and water can reach up to the order of 10^6 W/m^2 °C (Aya and Nariai, 1991). Typically, the steam is injected into a pool filled with subcooled water through a multi-hole sparger or single nozzle that is vertically or horizontally directed.

Condensation of steam can be categorized into four distinct regions. Firstly, a region named steam plume which consists of pure steam and is separated from the hot water layer by the steam water interface. Next is the hot water layer, which comprises water with steam bubbles and it is where condensation occurs primarily. The subcooled water surrounds the hot water layer (Petrovic de With et al., 2007).

The main thermohydraulic parameters governing DCC are the subcooling and the steam mass flux, with variations leading to different regimes.

For a single nozzle or sparger with one hole at low steam mass flux chugging (C) occurs. This condensation regime is characterized by a periodic formation and collapse of the steam plume resulting in the suction of water pool into the nozzle. With increasing steam mass flux, a regime was observed between chugging and condensation oscillation (CO) where the suction of the water pool no longer occurs named Transitional Chugging (TC). At higher steam mass flux, the steam-water interface starts to oscillate strongly (named condensation oscillation (CO)) until a stationary steam jet plume (named stable condensation (SC)) is established. At low water subcooling two condensation regimes are identified based on the steam mass flux. At low steam mass flux, the steam jet plumes detach from the nozzle and form isolated steam bubbles which can collapse or rise to the free surface. This regime is called bubbling condensation oscillation (BCO). Conversely, at high steam mass flux the condensation regime becomes highly unstable with a random changing of the steam jet plumes; it is named interfacial oscillation condensation (IOC) (Chun et al., 1996).

Chong et al., 2019 performed condensation tests at low mass flux using a horizontal nozzle having holes of 15–26 mm diameters. The experimental tests were performed at very small steam mass flux (about 20–40 kg/sm^2 for diameter of 26 mm and 30–120 kg/sm^2 for diameter of 15 mm). They observed three types of steam condensation regimes: chugging, hemispherical bubble oscillation and encapsulating bubble oscillation. During the chugging regime a steam bubble forms, growths and when it reaches a maximum volume the collapse occurs. This collapse causes the suction of the low subcooling water inside the pipe and the formation of an internal steam bubble that in turn generates the Condensation Induced Water Hammer (CIWH). This phenomenon occurs at a low steam mass flux (20 kg/sm^2) and low pool temperature (about 35 °C) with a hole diameter of 26 mm. When the temperature increases (at 65 °C) the encapsulating bubble oscillation occurs. Chong et al. observed three phases for the Encapsulating Bubble Oscillation (EBO): first the generation of a steam bubble and its growth around the pipe exit. After the necking, the bubble condenses and collapses rapidly. The location of the external bubble collapse does not induce a flow reversal. Its collapse causes pressure fluctuations of up to a maximum of 2.5 bar. During EBO, the steam bubble can become very large, encapsulating the pipe vent.

Youn et al., 2003 performed condensation experiments by injecting steam in a horizontal direction through a nozzle with diameters of 15–25 mm and steam mass flux between 10–80 kg/sm^2 and subcooling temperature of 30–80 °C. The aim of their work was to investigate the pressure oscillations due to direct contact condensation and obtain useful data for design purpose of the In-containment Refueling Water Storage Tank (IRWST). They measured the amplitude and the frequency of the pressure oscillations during the steam condensation and stated that the nozzle diameter influences the steam condensation regimes through the variation of steam jet interfacial area. It was observed that at low steam mass flux, the recorded pressure oscillations frequencies were low and could have induced the resonance of IRWST of the APR1400 reactor. The high-pressure oscillations were due to the detachment of steam bubbles.

The study of Kim and Choi, 2023 pointed out that the CIWH generated in a vertical pipe section results in a greater pressure shock compared to a horizontal pipe section confirming the needs for a deeper experimental investigation as proposed in the present paper.

The International Thermonuclear Experimental Reactor (ITER) implements a Vacuum Vessel Pressure Suppression System (VVPSS) to manage safely the Loss of Coolant Accident (LOCA) or Loss of Vacuum Accident (LOVA) ensuring that the Vacuum Vessel (VV) pressure remains below 1.5 bar. This is obtained by injecting through a multi-hole sparger the generated steam into four Vapour Suppression Tanks (VSTs), with a volume of 100 m^3 each, and therefore ensuring that the system remains at sub-atmospheric pressure condition. Three suppression tank named Large LOCA Tanks (LLTs) each containing 60 m^3 of water are designed to handle Category III and IV LOCA and LOVA events. Additionally, there is a Small LOCA Tank (SLT) with 40 m^3 of water to manage Category II events.

The study of the condensation phenomena in the case of adoption of a multi-hole sparger must account properly for the interactions between the neighboring steam jet plumes, the geometric factors of the sparger and the arrangement of the holes as well (Cho et al., 2004).

Cho et al., 2004 studied experimentally the performance of an I-type sparger. To this aim, different spargers with hole diameter of 5 mm, the ratio between the pitch and the hole diameter of 2–5, and two types of hole patterns, termed staggered and parallel, were tested. They observed that the dominant frequency of the pressure oscillations is high at low pool temperature (high subcooling) because the steam jet plumes break up into small bubbles that collapse very rapidly. Conversely, when the pool temperature increases (low subcooling) the steam bubble becomes bigger and the dominant frequency decreases. They noted that as the ratio between the pitch and the hole diameter decreases, the dominant frequency decreases because the neighboring steam plumes can combine to form a larger steam bubble.

Park et al., 2007 performed numerous condensation tests to assess the performance of a unit cell of the IRWST sparger.This cell had 64 holes with a diameter of 10 mm, arranged in 4 rows in a parallel hole pattern, with 50 mm pitch between holes in different rows and about 9 mm between holes in the same row. The tests were performed at high steam mass flux (from 190 to 600 kg/sm^2) and pool temperature between 20–95 °C. They measured the peak condensation loads at the tank bottom, finding that the loads increased when the steam mass flux decreased or the pool temperature increased up to 90 °C. Above 90 °C, the load decreases very rapidly.

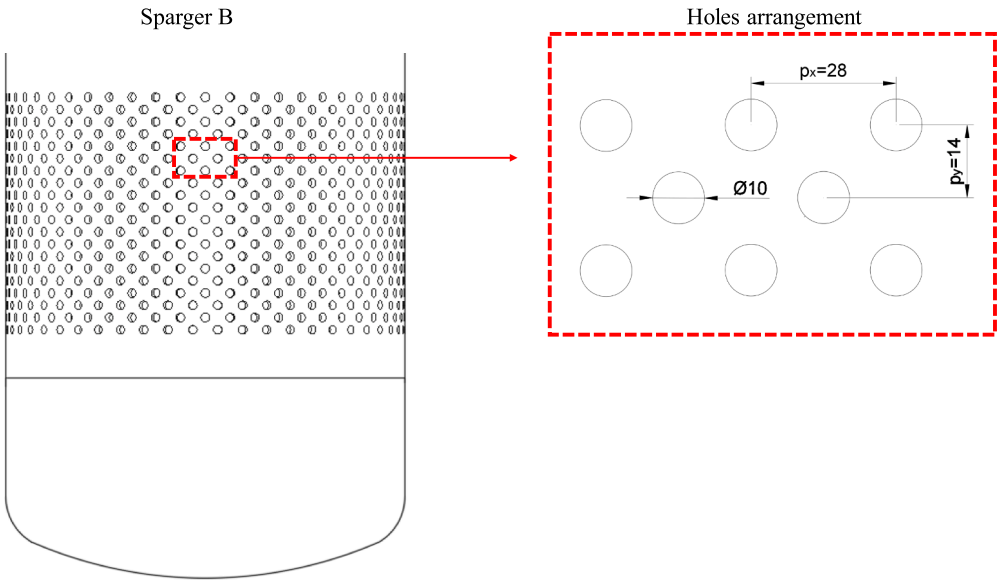

Fig. 1. Multi-hole and full-scale sparger B tested in the LSTF.

Zhang et al., 2023 performed condensation tests using a multi-hole sparger with 36 holes of 3 mm diameter in a parallel hole pattern with a pitch of 9 mm. During the tests, the coalescence of the steam jet plumes occurred when the subcooling pool temperature was at about 20 °C and for low steam mass flux (0–120 kg/s m^2).

With the aim to support the VVPSS qualification, numerous experimental tests have been performed in the recent years to study both the effects/consequences and the mechanism associated to the injection of steam, dust (Berti et al., 2023) and non-condensable gases (Berti et al., 2024a; Berti et al., 2024b) into a closed condensation tank under atmospheric and sub-atmospheric conditions. The extensive test campaign was funded by the ITER Organization.

A Small Scale Test Facility (SSTF) and a Large Scale Test Facility (LSTF) respectively, were designed and built. They installed different sparger prototypes.

During the tests on the LSTF, at low steam mass flux and low subcooling conditions, the steam jet plumes from each sparger hole coalesced resulting in a large steam bubble. The collapse of such a bubble generated on the structure high pressure loads at low frequency. To prevent such as a risk, a design methodology was developed. Based on the image analysis, which was conducted on 15 experimental tests (using the SSTF) featuring one single hole to evaluate the maximum steam plume radius under various steammass fluxes and pool subcooling conditions. A correlation was developed to predict it. Considering the full-scale sparger (or sparger B), two of its geometric bounds were defined in order to prevent a partial or the transition to the complete coalescence of the steam jet plumes and the consequent large bubble formation. The correlation was used in the analysis of data from tests under transient conditions for validation purposes.

2. Description of the facilities

At the University of Pisa, the above mentioned SSTF and LSTF experimental facilities were designed and constructed with the aim of qualifying the VVPSS. Both of them use a steam generator to deliver a maximum steam mass flow rate of 45 g/s and 500 g/s in a condensation tank (termed as CT101 and ETT for SSTF and LSTF, respectively) partially filled with subcooled water at sub-atmospheric pressure. The CT01 and ETT volume are 4.55 m^3 and 92 m^3 respectively. GoPro Hero 4 and GoPro Hero 7 cameras were used to capture videos of the experimental tests at a resolution of 1920 × 1080 pixels during testing execution with SSTF and LSTF, respectively.

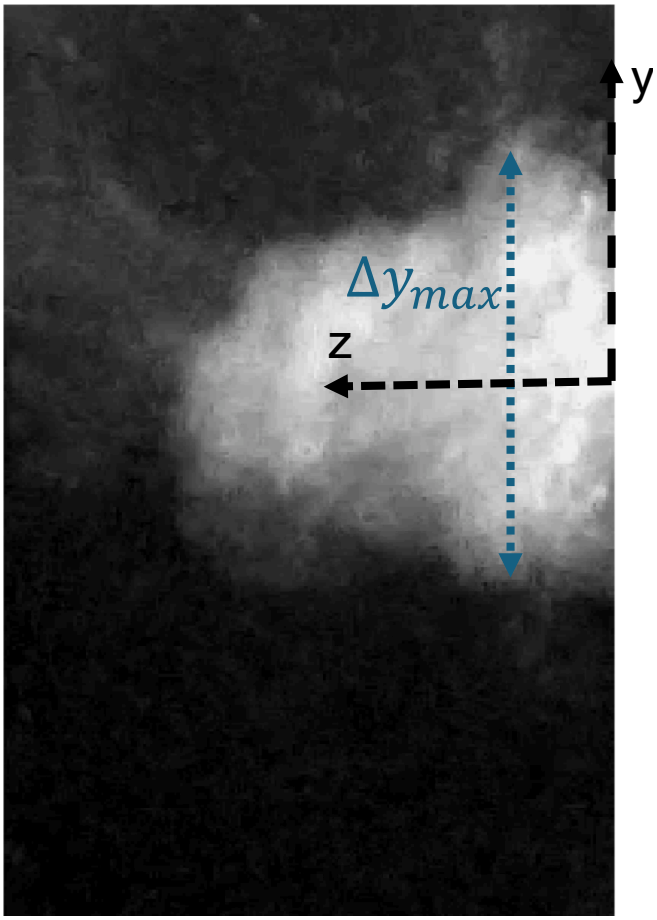

Fig. 2. Single steam jet plume for steam mass flux of 19 kg/sm^2 and subcooling temperature of 14.2 °C.

SSTF tested different spargers with 1–9 holes of 10 mm in diameter and different hole patterns (Mazed et al., 2018; Lo Frano et al., 2017). Meanwhile, LSTF tested two types of spargers, a reduced scale sparger

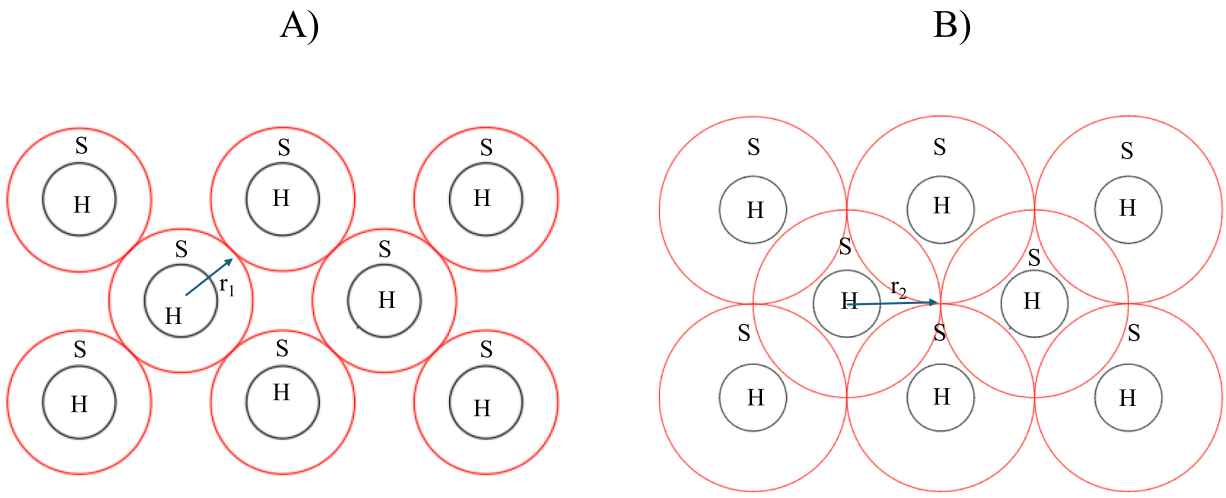

Fig. 3. Scheme of r_1 and r_2 for c = 2 (H = hole and S = steam).

with 100 holes and a full-scale one with 1000 holes (Aquaro and Pesetti, 2021; Pesetti et al., 2021; Berti et al., 2024; Giambartolomei et al., 2023).

Fig. 1 shows the sparger B tested in the LSTF: it consists of DN450 pipe with 1000 holes distributed in 20 rows around the pipe. The holes' arrangement features two different pitches: one between the holes of different rows (p_y) and another between the holes of the same row (p_x), as shown in Fig. 1. The ratio between p_x and p_y is about 2.

During the tests with sparger B a complete coalescence of the steam jet plumes occurred at 500 g/s of steam mass flow rate and low subcooling temperature (below 21 °C). Six video cameras recorded the steam condensation inside the ETT showing the development of big steam bubbles due to bubbles coalescence.

3. Design methodology

The Direct Contact Condensation (DCC) of the steam injected through one single hole at sub-atmospheric pressure condition was studied extensively at the University of Pisa by using SSTF. The data collected during these experimental tests were very useful to develop a predictive methodology of the conditions causing the steam coalescence when using a multi-hole sparger.

Kim and Lee, 1987 stated that the bubble coalescence occurs when two bubbles come into contact with each other in the liquid. Initially, a film separates them until its rupture forms the coalesced bubble. Therefore, an efficient methodology to avoid coalescence must be based on the separation of the steam plume jets of each hole.

Fig. 2 shows an example of the steam jet profile in SSTF with one single hole with steam mass flux of 19 kg/sm^2 and subcooling temperature of 14.2 °C. The image analysis of this test permits to calculate the maximum diameter (Δy_{max}) of the steam jet plume. This analysis was conducted utilizing ImageJ which is an open-source image processing program developed at the National Institute of Health (USA) (Schneider et al., 2012).

The calibration process for each videos captured by the camera was performed by evaluating the correspondence in mm of a pixel based on known dimensions of calibrated objects within the water pool.

Fifteen condensation tests, which were performed using a sparger with a single 10 mm hole, different steam mass flux (i.e. 20–31-61 kg/sm^2) and pool subcooling temperature 11–40 °C, were analyzed calculating for each test the maximum radius ($a_{max} = \Delta y_{max}/2$).

Taking into account the sparger B holes arrangement in a staggered pattern, we define the pitch ratio (c) as:

$$c = p_x/p_y \tag{1}$$

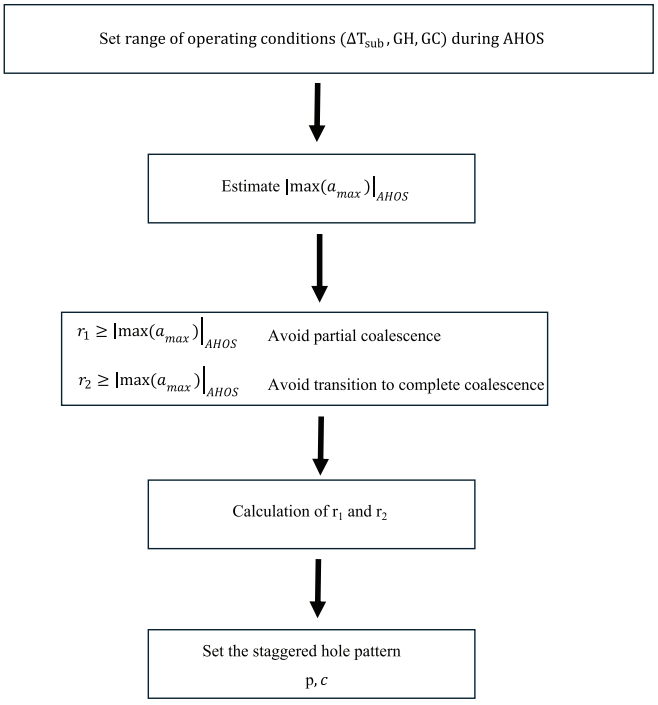

Fig. 4. Diagram of the design approach for sparger with staggered holes pattern in order to prevent partial and the transition to complete steam coalescence.

By assuming $p_y = p$ then

$$p_x = c \bullet p \tag{2}$$

Moreover let's call the two geometric bounds r_1 and r_2 respectively, then it follows:

$$r_1 = \sqrt{\frac{\left(\frac{p^2c^2}{4} + p^2\right)}{2}} \tag{3}$$

r_1 represents the condition for which the steam jet plumes are tangent each other. In this condition, the steam jet plumes of the same row do not interact. As for r_2, it is the condition for which the steam jet plumes of different rows coalesced and those of the same row are tangent. It is calculated as:

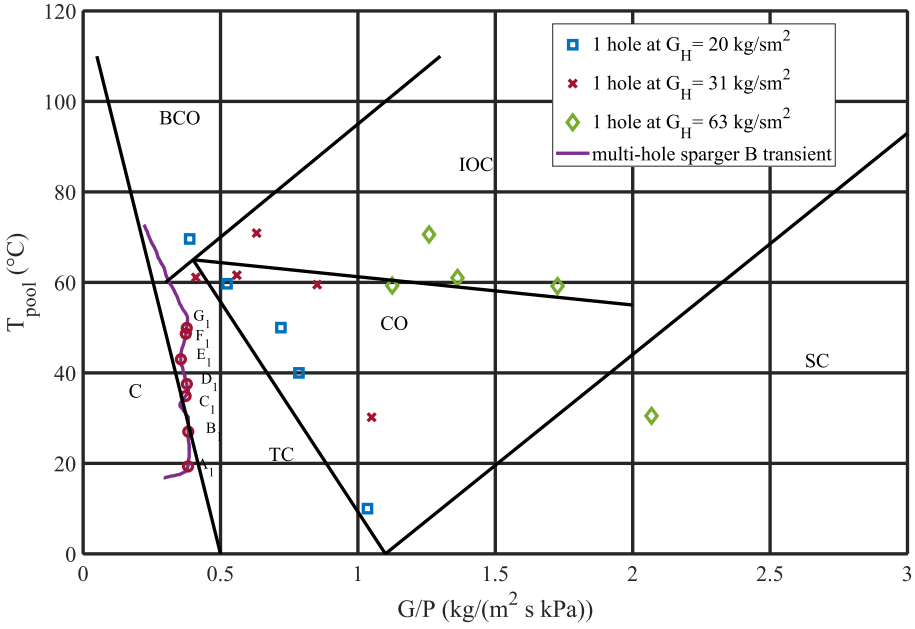

Fig. 5. Map of condensation regime for a single hole and multi-hole sparger considering no coalescence.

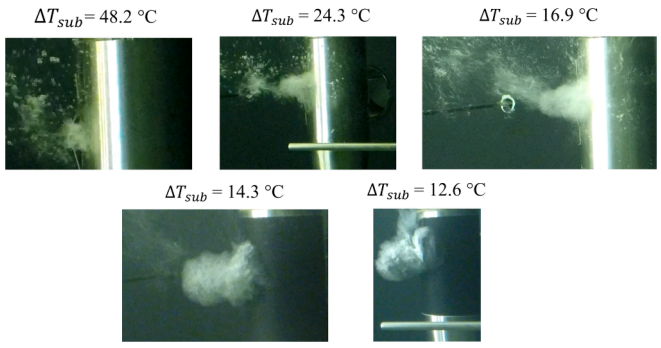

Fig. 6. Steam jet plumes at different ΔT_{sub} and for steam mass flux of 20 kg/ sm^2.

$$r_2 = \frac{c \bullet p}{2} \tag{4}$$

Pictures A) and B) of Fig. 3 show these bounds: the red circle represents the steam plume jet maximum circumference while the black one the sparger holes. r_1 and r_2 considering the sparger B geometry are equal to 9.9 mm and 14 mm respectively.

The value of a_{max} depends mainly by the steam mass flux and the critical steam mass flux through the single hole (named G_H and G_C, respectively) and the pool subcooling temperature ΔT_{sub}.

The variation ranges of ΔT_{sub}, G_H and G_C shall be established for all the hypothesized operating scenario (AHOS) in order to estimate the maximum value of a_{max} ($=|\max(a_{max})|_{AHOS}$).

Setting the value of p and c, the partial coalescence does not occur when $r_1 \geq a_{max}|_{AHOS}$. Instead, the transition to a complete coalescence of all the steam jet plumes is avoided when $r_2 \geq_{=} a_{max}|_{AHOS}$.

Fig. 4 shows the methodology for a sparger design with a staggered holes pattern: firstly, AHOS shall be established to fix the ranges of

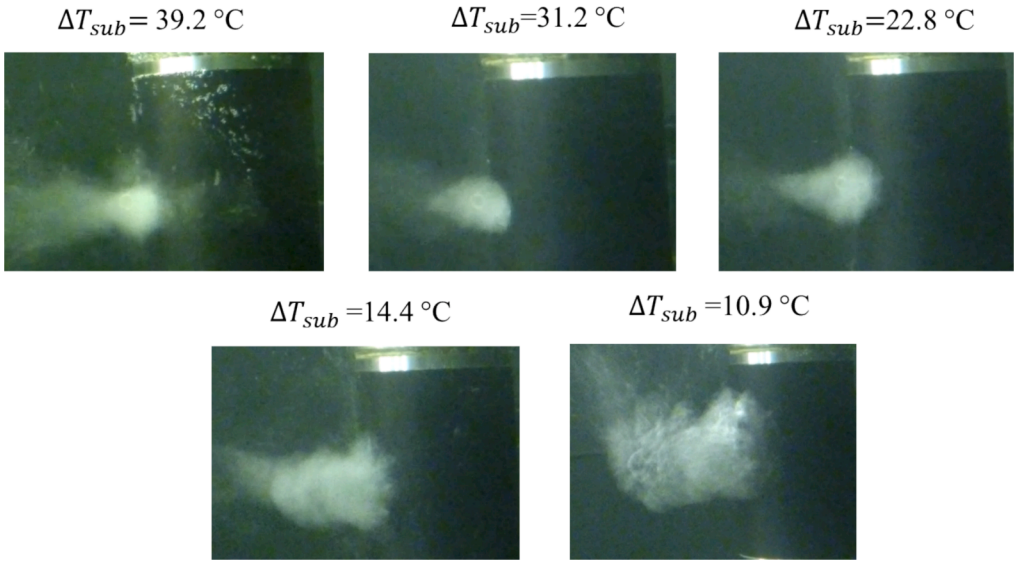

Fig. 7. Steam jet plumes at different ΔT_{sub} and for steam mass flux of 31 kg/sm^2.

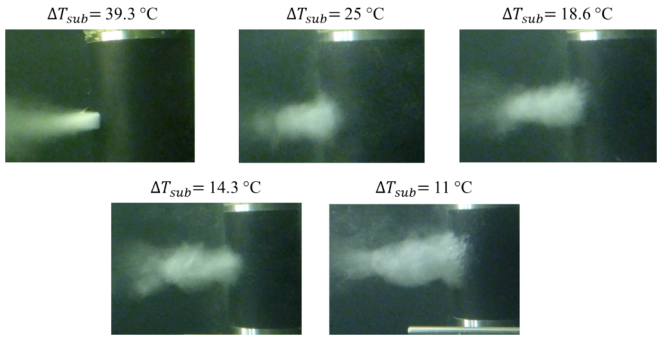

Fig. 8. Steam jet plumes at different ΔT_{sub} and for steam mass flux of 63 kg/s m^2.

ΔT_{sub}, G_H and G_C and subsequently max(a_{max})|$_{AHOS}$ is estimated. Secondly, p and c must be set in order to calculate r_1 and r_2. If these limits are respected the partial and the transition to complete coalescence can be avoided.

4. Results and discussion

This paper develops a methodology to design a multi-hole sparger with a staggered hole arrangement in order to prevent coalescence at sub-atmospheric conditions. If the coalescence is not prevented, a steam bubble with a very large volume depending on the steam mass flow rate can form. The collapse of such bubbles after the detachment may generate a large pressure load on the structure. Larger steam bubbles produce higher pressure loads so it is important to limit their volumes as much as possible.

The image analysis aimed to measure the maximum radius of the steam jet plume at different subcooling temperature and different steam mass flux. Fig. 5 shows a condensation regime map (Mazed et al., 2018) based on data from 400 tests.

The analyzed experimental tests (for 20–63 kg/sm^2 steam mass flux and 11–48 °C subcooling temperature) with one hole are indicated in the map: low steam mass fluxes determine unstable regimes as CO, IOC, BCO and TC. Only one test is in stable condensation (SC).

Figs. 6, 7 and 8 show the steam jet plumes for the 15 analysed tests. It is worth noting that as ΔT_{sub} decreases, a_{max} increases due to the reduction in condensation rate. Conversely, for the same ΔT_{sub} increasing the steam mass flux a_{max} decreases.

As already said in the previous section, the coalescence can be avoided by maintaining separate the steam jet plumes of each hole. Considering the experimental values of a_{max}, it was developed a correlation which permits to estimate the ratio between a_{max} and the hole diameter (D_H). This correlation is function of the condensation driving potential (B), critical steam mass flux (G_c), and steam mass flux through one hole (G_H) and can be written as:

$$\frac{a_{max}}{D_H} = 0.0596\, B^{-0.94} \left(\frac{G_H}{G_C}\right)^{-0.211} \tag{5}$$

Where:

$$B = c_p \frac{\Delta T_{sub}}{h_{fg}} \tag{6}$$

$$Gc = C_D \left[p_0 \rho_0 \gamma \left(\frac{2}{\gamma+1}\right)^{\frac{\gamma+1}{\gamma-1}} \right]^{\frac{1}{2}} \tag{7}$$

In the above Equation (6) and Equation (7), c_p is the water specific heat capacity, h_{fg} is the latent heat of vaporization, C_D is the efflux coefficient assumed to be equal to 1, p_0 is the steam pressure, ρ_0 is the steam density and γ is the ratio between the specific isobaric and isochoric heat capacity of steam. The variation in condensation rate is accounted for by the parameter B while the steam velocity and the pressure near holes is represented by the ratio G_H/G_C.

Fig. 9 shows the comparison between the measured maximum radius at different ΔT_{sub} (between 10–45 °C) and steam mass flux (between 20–61 kg/s m^2) with that obtained from the correlation at constant steam critical flux and D_h equals to 10 mm. The error bar corresponds to one standard deviation with respect to the average maximum radius.

The maximum radius of the steam jet plumes was determined by considering a statistically meaningful number of frames depending on the condensation regimes.

As the pool subcooling temperature decreases, the condensation rate decreases resulting in an increase in the a_{max}. This occurs because the steam jet plumes need to expand to increase the interfacial surface area

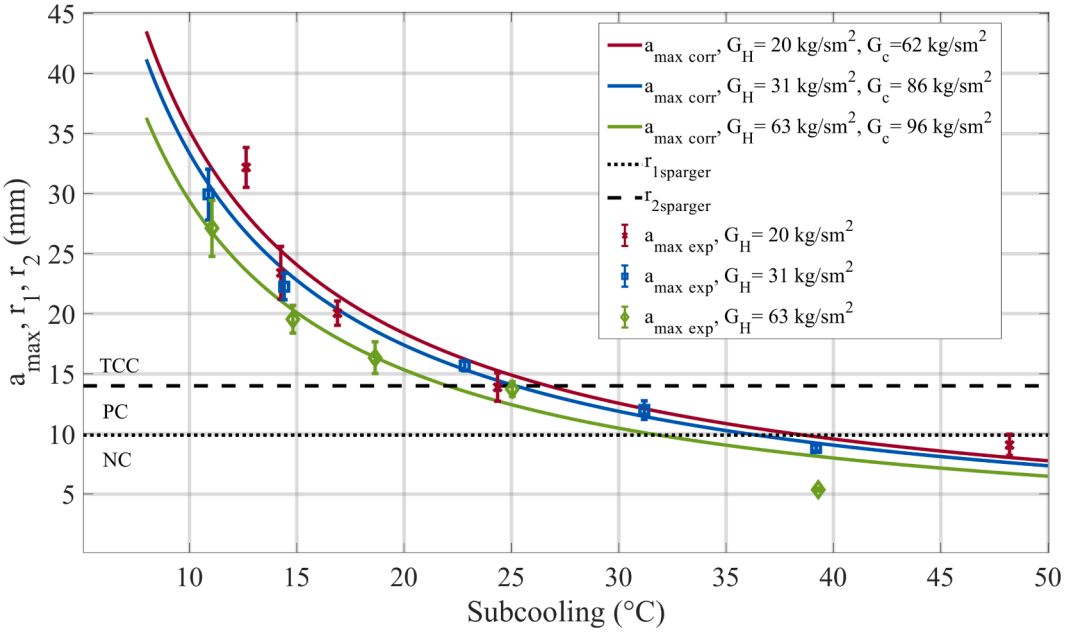

Fig. 9. Experimental (exp) and correlation (corr) steam jet plumes maximum radius.

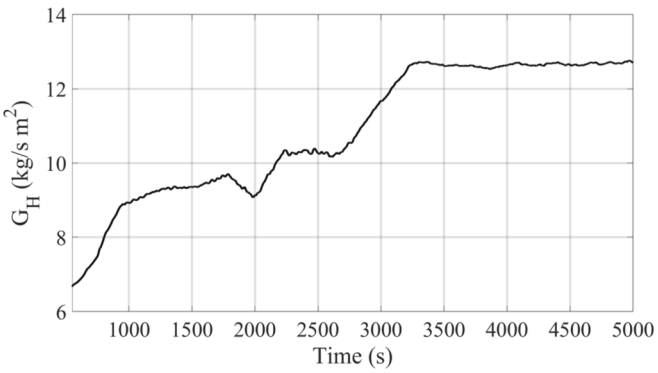

Fig. 10. Steam mass flux during test under transient conditions.

between the steam and water.

As the steam mass flux increases, the length of the steam jet plume increases, thereby reducing a_{max}.

The maximum error in a_{max} predictions using the correlation of Eq. (5) calculated with respect to the average experimental a_{max} is about 6 % when the condensation regime is condensation oscillation or transitional chugging except at high subcooling (48 °C) when the error becomes 11 %. 10 % error is calculated for the bubbling condensation oscillation (BCO).

At steam mass flux of 63 kg/sm^2 and $\Delta T_{sub} = 39$ °C, the condensation regime is stable and a_{max} is equal to the radius of the hole. In this case the correlation cannot be applied. The comparison between a_{max} and r_1 and r_2 allow to define three regions: the non-coalescence region (NC), the partial coalescence region (PC) and the transitional complete coalescence region (TCC).

In the NC region, when $r_1 \geq a_{max}$, the sparger multi-hole design ensures separation of the steam jet plumes from each hole.

The PC region occurs when $r_1 \leq a_{max}$, and causes some steam jet plumes to start coming into contact, forming isolated steam pockets that can collapse. As a_{max} approaches r2, the number of interacting steam jet plumes increases.

The TCC represents a transitional region between the partial and the complete coalescence (CC) regions. Periodically, all the steam jet plumes interact forming an isolated steam bubble, while in other cycles, only some jet plumes interact forming isolated steam pockets.

In the Fig. 9, the values of r_1 and r_2 for sparger B are indicated as generic example to show, as a function of these values, the different regions NC, PC and TC.

The correlation was then applied to data from test under transient condition performed using sparger B, steam mass flux between 6.67–12.73 kg/sm^2, as shown in Fig. 10, and ΔT_{sub} between 14–50 °C, as shown in Fig. 11.

Fig. 11 shows the variation of a_{max} during the transient taken into account an error of ± 10 %. The injection of steam inside the pool water increases the water temperature decreasing the pool subcooling from 50 °C to 14 °C. For this reason, a_{max} increases until it reaches r_1 and r_2 (points B_1 and E_1 in the Fig. 11).

The images A_1, B_1 and C_1 in Fig. 12 and Fig. 13 illustrate the correspondence of test time when a_{max} + 10 %, a_{max} and a_{max} − 10 % are equal to r_1. The image confirms that some steam plume jets are tangent, but no steam coalesced pocket is formed with sparger B when the water subcooling temperature ranges between 37–45 °C and the steam mass flux is about 9.21 kg/sm^2, except some coalescence of few holes in the bottom region. This is the NC region.

The image D1, E1 and F1 in Fig. 12 and Fig. 13 show the test time

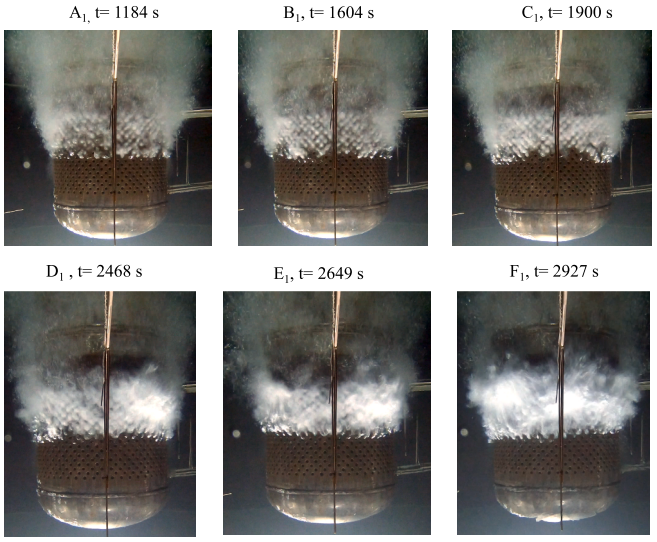

Fig. 12. Maximum steam pocket when a_{max} ± 10 % is equal to r_1 (A_1, B_1, C_1) and r_2 (D_1, E_1, F_1).

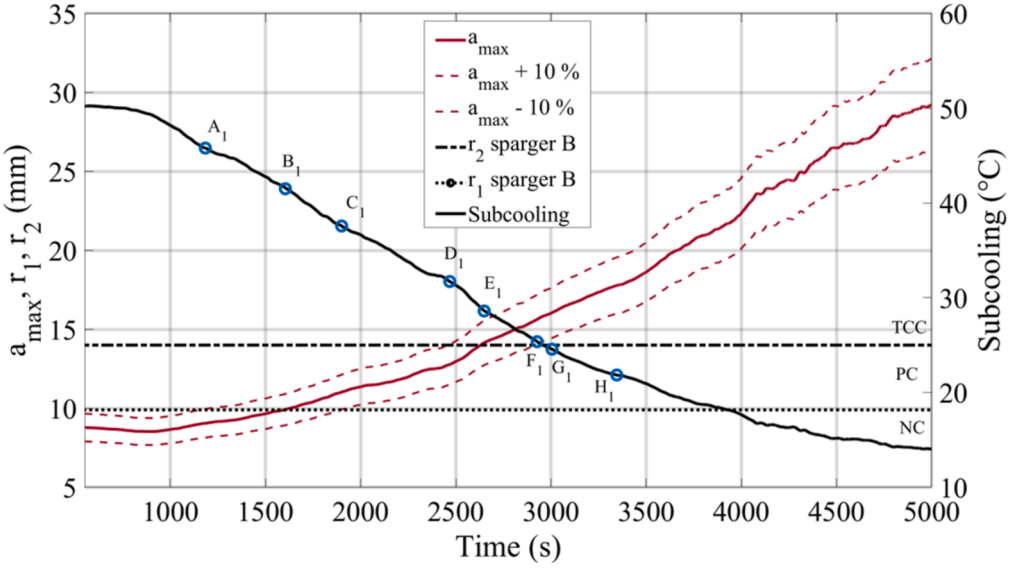

Fig. 11. a_{max} during transient test performed with sparger B (c = 2).

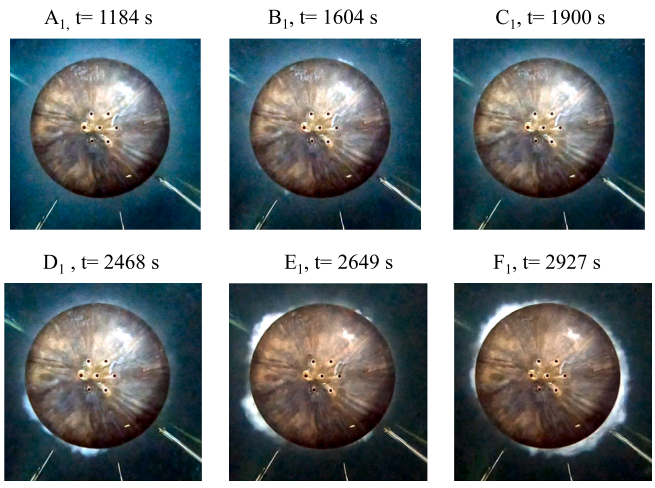

Fig. 13. Sparger bottom view: maximum steam pocket when $a_{max} \pm 10$ % is equal to r_1 (A_1, B_1, C_1) and r_2 (D_1, E_1, F_1).

when $a_{max} + 10$ %, a_{max} and $a_{max} - 10$ % are equal to r_2. A partial coalescence is evident, while some jet plumes form a steam pocket, others do not coalesce simultaneously for subcooling ranging from 25° to 31 °C. This prevents the formation of a single steam bubble with a larger volume but results in higher pressure loads than the non-coalescence region.

As a_{max} becomes larger than r_2, the transition to complete coalescence region starts: this region is the TCC. In this region, the partial and complete coalescence of the steam jet plumes alternate; initially, the partial coalescence predominates, and gradually, the complete coalescence becomes prevalent.

Fig. 14 shows the bubble dynamics at point G_1 when the water subcooling is 24.57 °C and a_{max} is beyond r_2. A steam bubble grows, reaches a maximum volume, detaches and collapses between 3005.12 s and 3005.4 s.

The complete coalescence region starts at about 3345 s when the subcooling temperature is about 21 °C in the point H_1. In this region, the complete coalescence of the steam jet plumes occurs cycling. Fig. 15 shows the bubble dynamics in this region, all the steam jet plumes coalesce to form a large steam bubble which detaches and collapses resulting in large pressure loads on the structure. In this case, the average a_{max} is 17.77 mm that is about 4 mm above r_2.

These results show that if the geometric bounds (limit conditions) are respected, PC and TCC regions can be avoided by decreasing the pressure load due to the external steam bubbles collapse and by avoiding the associated flow reversal, which can develop additional internal pressure loads due to the CIWH.

5. Conclusions

In this study, a methodology to prevent the steam coalescence and in turn limit the pressure loads acting on the structure, by using a multi-hole sparger at low steam mass flux was described and critically discussed.

An image analysis of 15 experimental tests at the SSTF and with a

Fig. 14. Bubble dynamics (point G_1) when $a_{max} + 10$ % is beyond r_2 in the region TCC.

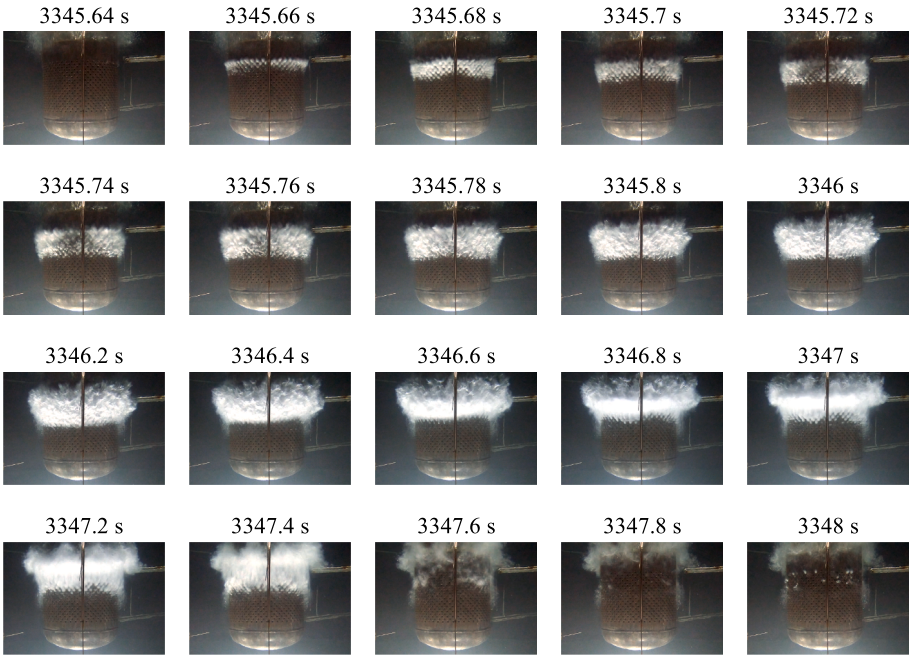

Fig. 15. Bubble dynamics (point H_1) when a_{max} + 10 % is beyond the limit r_2 in the region CC.

single hole sparger was performed using an open-source software in order to develop a correlation, as a function of the condensation driving potential, the steam mass flux and the critical steam mass flux, capable to predict the ratio between the maximum radius of the steam jet plumes and the hole diameter.

The outcomes show that as subcooling decreases, a_{max} increases and as steam mass flux increases, a_{max} decreases.

Based on that, two geometrical bounding conditions have been defined, with reference to the maximum radius that allow to prevent partial or the transition to the complete coalescence of the steam jet plumes; for the specific design of ITER sparger, r_1 and r_2 are 9.9 mm and 14 mm, respectively.

The validation of the proposed methodology was done by applying the correlation to a test under transient conditions performed with a full scale VVPSS multi-holes sparger and analyzing the recordings from the cameras.

The correlation estimates that PC and TCC are prevented when the water subcooling temperature ranges between 37–45 °C and 25–31 °C, respectively, as observed in the recordings of the cameras.

Moreover, the recordings showed that as the subcooling decreases below 25 °C, the transition to complete coalescence starts and continueuntil complete coalescence is achieved below 21 °C.

The analysis shows that if the limits are respected, PC and TCC regions can be avoided limiting the pressure loads on multi-hole sparger and demonstrates that the methodology can be effectively applied to design multi-hole spargers to mitigate steam coalescence and associated high-pressure loads.

CRediT authorship contribution statement

Luca Berti: Writing – original draft, Visualization, Software, Methodology, Investigation, Formal analysis, Data curation, Conceptualization. **Donato Aquaro:** Writing – review & editing, Supervision. **Rosa Lo Frano:** Writing – review & editing, Supervision.

Declaration of competing interest

The authors declare that they have no known competing financial interests or personal relationships that could have appeared to influence the work reported in this paper.

Acknowledgments

This experimental study was carried out thanks to the ITER Organization support (service contract: IO/17/CT/4300001491), to which the authors express their grateful acknowledgement. The authors wish to thank all the DICI technicians involved.

Disclaimer

The views and opinions expressed herein do not necessarily reflect those of the ITER Organization.

Data availability

The data that has been used is confidential.

References

Aquaro, D., Pesetti, A., 2021. Experimental qualification of the ITER pressure suppression system by means of a large scale facility: Assessment of similitude analysis. Nucl. Fusion 61 (12), 126010.

Aya, I., Nariai, H., 1991. Evaluation of heat-transfer coefficient at direct-contact condensation of cold water and steam. Nucl. Eng. Des. 131 (1), 17–24.

Berti, L., Aquaro, D., Raucci, M., Pesetti, A., 2023. Dust produced by plasma off normal event in the vacuum vessel: Experimental analyses of the deposition inside the pressure suppression tank during a LOCA. Fusion Eng. Des. 190, 113540.

Berti, L., Pesetti, A., Raucci, M., Giambartolomei, G., Aquaro, D., 2024a. Influence of noncondensable gas-dust mixture on direct contact condensation of steam at atmospheric pressure. J. Nucl. Eng. Radiat. Sci. 10 (1), 012301.

Berti, L., Pesetti, A., d'Errico, F., Aquaro, D., 2024b. Structural and thermal fluid dynamics analyses of the ITER Pressure Suppression System considering no stable steam condensation regimes. Fusion Eng. Des. 201, 114305.

Cho, S., Chun, S.-Y., Baek, W.-P., Kim, Y., 2004. Effect of multiple holes on the performance of sparger during direct contact condensation of steam. Exp. Therm Fluid Sci. 28 (6), 629–638.

Chong, D., Xiaoyu, Y., Wang, L., Zhao, Q., Yan, J., 2019. Experimental investigation on condensation patterns and pressure oscillation characteristics of steam submerged jet through a horizontal pipe at low steam mass flux. Int. J. Heat Mass Transf. 139, 648–659.

Chun, M.-H., Kim, Y.-S., Park, J.-W., 1996. "An investigation of direct condensation of steam jet in subcooled water. Int. Commun. Heat Mass Transfer 23 (7), 947–958.

Giambartolomei, G., Pesetti, A., Berti, L., Raucci, M., Lazzeri, R., Aquaro, D., 2023. Reverse flow in a pressure suppression system due to condensation instabilities. J. Phys. Conf. Ser. 2509.
Kim, M., Choi, S., 2023. Numerical investigation of condensation-induced water hammer effects in horizontal and vertical cold reheat pipes. Int. J. Heat Mass Transf. 207, 124030.
Kim, J.W., Lee, W.K., 1987. Coalescence behavior of two bubbles in stagnant liquids. J. Chem. Eng. Jpn. 20 (5), 448–453.
Lo Frano, R., Mazed, D., Aquaro, D., Del Serra, D., Orlandi, F., 2017. Experimental investigation of functional performance of a vacuum vessel pressure suppression system of ITER. Fusion Eng. Des. 122, 42–46.
Mazed, D., Lo Frano, R., Aquaro, D., Del Serra, D., Sekachev, I., Olcese, M., 2018. Experimental investigation of steam condensation in water tank at sub-atmospheric pressure. Nucl. Eng. Des. 335, 241–254.
Park, C.K., Song, C.H., Jun, H.G., 2007. Experimental investigation of the steam condensation phenomena due to a multi-hole sparger. J. Nucl. Sci. Technol. 44 (4), 548–557.
Pesetti, A., Marini, A., Raucci, M., Giambartolomei, G., Olcese, M., Sarkar, B., Aquaro, D., 2021. Large scale experimental facility for performance assessment of the vacuum vessel pressure suppression system of ITER. Fusion Eng. Des. 171, 112523.
Petrovic de With, A., Calay, R.K., de With, G., 2007. Three-dimensional condensation regime diagram for direct contact condensation of steam injected into water. Int. J. Heat Mass Transf. 50 (9–10), 1762–1770.
Schneider, C.A., Rasband, W.S., Eliceiri, K.W., 2012. NIH Image to ImageJ: 25 years of image analysis. Nat. Methods 9, 671–675.
Youn, D.H., Ko, K.B., Lee, Y.Y., Kim, M.H., Bae, Y.Y., Park, J.K., 2003. The direct contact condensation of steam in a pool at low mass flux. J. Nucl. Sci. Technol. 40 (10), 881–885.
Zhang, D., Tong, L., Cao, X., 2023. Condensation Oscillation characteristic of steam with non-condensable gas through multi-hole sparger at low mass flux. Nucl. Eng. Technol. 55 (2), 780–791.